Probing the Role of the Histidine 759 Ligand in Cobalamin−Dependent Methionine Synthase †

ARTICLE *in* BIOCHEMISTRY · AUGUST 2007

Impact Factor: 3.02 · DOI: 10.1021/bi700341y · Source: PubMed

4 AUTHORS:

Matthew D Liptak
University of Vermont
21 PUBLICATIONS **1,319** CITATIONS
SEE PROFILE

Angela S Fleischhacker
University of Michigan
11 PUBLICATIONS **175** CITATIONS
SEE PROFILE

Rowena Green Matthews
University of Michigan
172 PUBLICATIONS **13,394** CITATIONS
SEE PROFILE

Thomas C Brunold
University of Wisconsin−Madison
102 PUBLICATIONS **3,915** CITATIONS
SEE PROFILE

Probing the Role of the Histidine 759 Ligand in Cobalamin-Dependent Methionine Synthase†

Matthew D. Liptak,‡,§ Angela S. Fleischhacker,‡,|| Rowena G. Matthews,||,⊥ and Thomas C. Brunold*,§

Department of Chemistry, University of Wisconsin—Madison, Madison, Wisconsin 53706, and Department of Chemistry and Life Sciences Institute, Department of Biological Chemistry, and Biophysics Research Division, University of Michigan, Ann Arbor, Michigan 48109

Received February 17, 2007; Revised Manuscript Received April 18, 2007

ABSTRACT: Cobalamin-dependent methionine synthase (MetH) of *Escherichia coli* is a 136 kDa, modular enzyme that undergoes large conformational changes as it uses a cobalamin cofactor as a donor or acceptor in three separate methyl transfer reactions. At different points during the reaction cycle, the coordination to the cobalt of the cobalamin changes; most notably, the imidazole side chain of His759 that coordinates to the cobalamin in the "His-on" state can dissociate to produce a "His-off" state. Here, two distinct species of the cob(II)alamin-bound His759Gly variant have been identified and separated. Limited proteolysis with trypsin was employed to demonstrate that the two species differ in protein conformation. Magnetic circular dichroism and electron paramagnetic resonance spectroscopies were used to show that the two species also differ with respect to the axial coordination to the central cobalt ion of the cobalamin cofactor. One form appears to be in a conformation poised for reductive methylation with adenosylmethionine; this form was readily reduced to cob(I)alamin and subsequently methylated [albeit yielding a unique, five-coordinate methylcob(III)alamin species]. Our spectroscopic data revealed that this form contains a five-coordinate cob(II)alamin species, with a water molecule as an axial ligand to the cobalt. The other form appears to be in a catalytic conformation and could not be reduced to cob(I)alamin under any of the conditions tested, which precluded conversion to the methylcob(III)alamin state. This form was found to possess an effectively four-coordinate cob(II)alamin species that has neither water nor histidine coordinated to the cobalt center. The formation of this four-coordinate cob(II)alamin "dead-end" species in the His759Gly variant illustrates the importance of the His759 residue in governing the equilibria between the different conformations of MetH.

Cobalamin-dependent methionine synthase (MetH)[1] from *Escherichia coli* catalyzes the conversion of homocysteine (Hcy) to methionine (Met) as the final step in the de novo biosynthesis of Met (Scheme 1). MetH is a 136 kDa enzyme composed of four functionally distinct modules that are arranged linearly with single interdomain linkers (*1*). The N-terminal module binds and activates Hcy, while the second module binds and activates methyltetrahydrofolate (CH_3-H_4-folate). The third module binds the cobalamin (Cbl) cofactor in such a way that the dimethylbenzimidazole base that acts as the α-ligand (i.e., "lower" axial ligand) to the cobalt in the free cofactor is replaced by the imidazole side chain of His759. Finally, the last module is necessary for the reductive methylation of MetH, as it binds and activates adenosylmethionine (AdoMet) and contains surface residues implicated in the binding of flavodoxin (Fld) (*2*−*4*).

Scheme 1

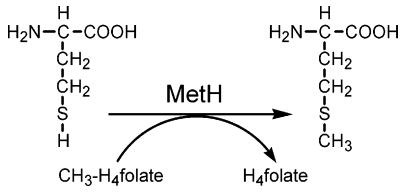

Both catalytic substrate-binding modules interact with Cbl during the methyl transfer reactions (Figure 1). However, inspection of all available X-ray crystal structures of MetH reveals that, at any given time, the Cbl-binding module is in contact with only one other module, suggesting that MetH

† This work was supported by the National Science Foundation (CAREER Grant MCB-0238530 to T.C.B.) and the National Institutes of Health (Grant GM29408 to R.G.M.).

* To whom correspondence should be addressed: phone, (608) 265-9056; fax, (608) 262-6143; e-mail, Brunold@chem.wisc.edu.

‡ These two authors have contributed equally to this work.

§ Department of Chemistry, University of Wisconsin—Madison.

|| Department of Chemistry, University of Michigan.

⊥ Life Sciences Institute, Department of Biological Chemistry, and Biophysics Research Division, University of Michigan.

[1] Abbreviations: Abs, electronic absorption; AdoMet, adenosylmethionine; Cbl, cobalamin; CH_3-H_4folate, methyltetrahydrofolate; Co^{1+}-Cbl, cob(I)alamin; Co^{1+}Cbl(act), Co^{1+}Cbl-bound wild-type MetH in the reactivation conformation; Co^{1+}Cbl(cat), Co^{1+}Cbl-bound wild-type MetH in the catalytic conformations; $Co^{2+}Cbi^{+}$, cob(II)inamide; Co^{2+}-Cbl, cob(II)alamin; DFT, density functional theory; EPR, electron paramagnetic resonance; Fld, flavodoxin; FPLC, fast protein liquid chromatography; H759G, His759Gly mutant; H759G(act), Co^{2+}Cbl-bound H759G MetH in the reactivation conformation; H759G(cat), Co^{2+}Cbl-bound H759G MetH in the catalytic conformations; H759G-(met), MeCbl-bound H759G MetH; HCl, hydrochloric acid; Hcy, homocysteine; MCD, magnetic circular dichroism; $MeCbi^{+}$, methylcobinamide; MeCbl, methylcob(III)alamin; Met, methionine; MetH, cobalamin-dependent methionine synthase; MOs, molecular orbitals; SOMO, singly occupied molecular orbital; TLCK, tosyl lysyl chloromethyl ketone.

10.1021/bi700341y CCC: $37.00
Published on Web 06/13/2007

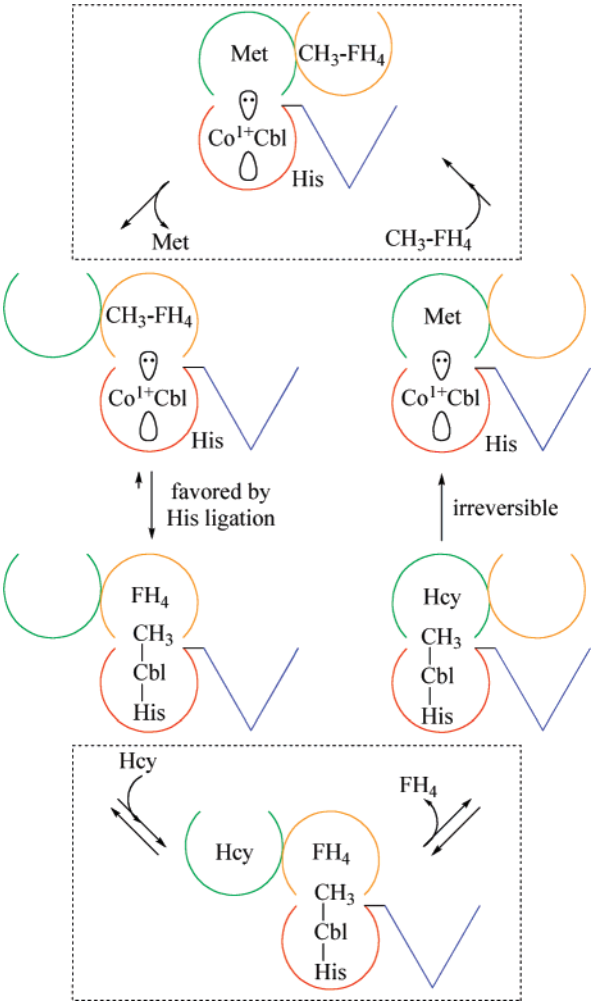

FIGURE 1: Schematic representation of the catalytic cycle of MetH. The four modules of MetH are colored green (Hcy-binding), gold (CH_3-H_4-folate-binding), red (Cbl-binding), and blue (AdoMet-binding; used for reactivation). The Hcy- and CH_3-H_4folate-binding modules are rigidly fixed with respect to one another, and only one of these two modules can interact with the Cbl at any given time, requiring large conformational changes to provide the Cbl access to the two different substrates during turnover. Substrate binding and product release can only occur on the module that is not interacting with the Cbl-binding module; the dotted boxes show the conformation formed after substrate binding and prior to the conformational change required for product release. Methyl transfer from MeCbl to Hcy to form Met and Co^{1+}Cbl is irreversible (*6*), while transfer from MeCbl to tetrahydrofolate (FH_4) is reversible.

undergoes large conformational changes during catalysis (*5*). In the MetH catalytic cycle shown in Figure 1, the methyl group of methylcob(III)alamin (MeCbl) is transferred to Hcy to form Met and cob(I)alamin (Co^{1+}Cbl); the latter form of the cofactor is subsequently remethylated with CH_3-H_4folate (*6*). During the catalytic cycle, Cbl is presumed to alternate between His-on MeCbl and His-off Co^{1+}Cbl states as it is successively demethylated and remethylated. The Co^{1+}Cbl generated in this process is susceptible to oxidation to the catalytically inactive cob(II)alamin (Co^{2+}Cbl) state under aerobic conditions (*2*). The enzyme reactivates this Co^{2+}-Cbl species to the catalytically active MeCbl state through reductive methylation using reduced Fld as the electron donor and AdoMet as the source of the methyl group (*7*−*9*). Binding of Fld to MetH containing Co^{2+}Cbl, which is initially in a His-on conformation as judged by its electron paramagnetic resonance (EPR) spectrum, leads to the dissociation of the His759 ligand to yield a His-off species (*10*, *11*).

To obtain deeper insight into the catalytic and reactivation cycles of MetH, the His759Gly (H759G) mutant, in which the cofactor is forced to adopt a His-off conformation, was prepared and characterized. This variant has been shown to be active in reductive methylation but not in catalytic turnover (*12*). The Co^{2+}Cbl-bound state of H759G MetH also showed a marked difference from the wild-type enzyme in its cleavage pattern upon limited proteolysis of the native enzyme with trypsin (*13*). These observations suggested that the H759G mutant, and by analogy the His-off form of Co^{2+}-Cbl-bound wild-type MetH, is in a different conformation than the His-on form of the native enzyme. The key structural features of this different conformation can be inferred from the X-ray crystal structure of a truncated H759G variant of MetH (residues 649−1227) that contains only the Cbl- and AdoMet-binding modules (*14*). This structure revealed that the truncated variant protein adopts a conformation in which the AdoMet-binding module interacts with the Cbl-binding module. This conformation of the protein is thus poised for reductive methylation with AdoMet and is therefore referred to as the reactivation conformation (Figure 2). A unique feature of this conformation is that a loop from the AdoMet-binding module is situated between the corrin ring and the Cbl-binding module, suggesting that in wild-type MetH a similar interaction serves to force the Cbl cofactor into the His-off coordination mode. In order to avoid futile cycling, interconversion between the reactivation conformation and the catalytic conformations is strictly regulated; in particular, enzyme containing the cofactor in the Co^{1+}Cbl state is unable to interconvert between these two conformations. Hence, Co^{1+}Cbl generated during reductive methylation is only able to react with AdoMet, while Co^{1+}Cbl generated by demethylation with Hcy is only able to react with CH_3-H_4-folate (*13*).

Since MetH-bound Co^{1+}Cbl, which is always His-off, cannot interconvert between the reactivation conformation and the catalytic conformations, it is of considerable interest to know the precise coordination mode of MetH-bound MeCbl and Co^{2+}Cbl in their His-off forms. A series of electrochemical studies, summarized by Lexa and Saveant, have revealed that in aqueous solution the coordination numbers of the Co center in base-off MeCbl and Co^{2+}Cbl are six and five, respectively, with water bound to an axial coordination site (*15*). However, prior to the present study, it was not clear whether His-off Cbl retained this axial water molecule in the MetH active site. Furthermore, it remained unknown whether the cofactor in the H759G mutant, which is obligatorily His-off, would have the same axial ligation in the catalytic and reactivation conformations of the enzyme. Finally, since the H759G mutant no longer has the His759 ligand that, by coordinating to the Co center, may aid in driving the catalytic cycle and/or the conformational switch between the reactivation and catalytic conformations, one might expect these processes to be strongly perturbed from wild-type behavior.

Recently, we have employed magnetic circular dichroism (MCD) and EPR spectroscopic techniques to probe the axial coordination environment of the Co center in MeCbl and Co^{2+}Cbl (*16*, *17*). These studies have revealed that a

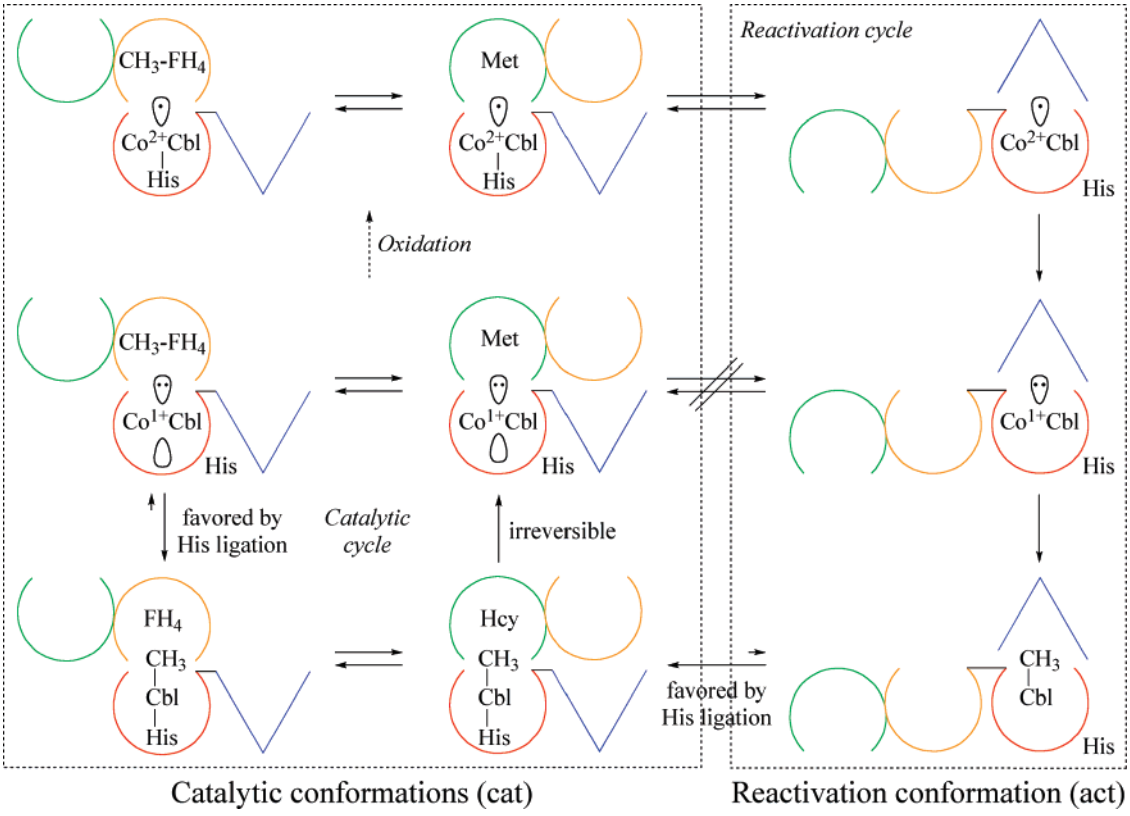

FIGURE 2: Schematic representation of the catalytic and reactivation cycles of MetH. The scheme depicting catalytic turnover (lower left) has been simplified by omitting the substrate-binding and product-release steps, steps contained in the boxes in Figure 1. As indicated in this figure by the dashed arrow, the Co^{1+}Cbl cofactor becomes oxidized about once in every 2000 turnovers (*26*), yielding a Co^{2+}Cbl species that is in the His-on form. Addition of Fld results in a switch to His-off Co^{2+}Cbl and conversion from a catalytic conformation (dotted box on the left) to the reactivation conformation (dotted box on the right). Following electron transfer from reduced Fld and methyl transfer from AdoMet, His-off MeCbl is formed. The subsequent conversion to His-on MeCbl with MetH in a catalytic conformation is the rate-limiting step in the reductive methylation reaction (*11*). As indicated by the broken arrows, enzyme in the Co^{1+}Cbl-bound form is unable to interconvert between catalytic and reactivation conformations (*13*).

perturbation of the axial coordination environment has virtually no effect on the relative energies of the corrin π-/π*-based molecular orbitals (MOs) but a rather large effect on the Co 3d-based MOs. In both MeCbl and Co^{2+}Cbl, the perturbation of the Co 3d-based MOs causes a shift in the peak position of the first observed electronic transition. This peak position is more precisely established via MCD spectroscopy than the more traditional electronic absorption (Abs) spectroscopy due to the increased resolution of individual electronic transitions inherent to a signed spectrum. Furthermore, in the case of Co^{2+}Cbl the relative intensity of this transition is several orders of magnitude larger in the MCD spectrum than in the Abs spectrum since it involves MOs with predominant Co 3d character, thus ensuring large spin−orbit mixing with ligand-field transitions (*18*).

In this work, two distinct species of the Co^{2+}Cbl-bound H759G MetH mutant have been identified and separated by fast protein liquid chromatography (FPLC). The two species differ in their ability to catalyze the reductive methylation of the cofactor and are locked into different enzyme conformations, as revealed by limited proteolysis. Specifically, one of the H759G mutant species is in the reactivation conformation (i.e., with the AdoMet-binding module in close contact with the Cbl-binding module), while the other is in a conformation utilized for catalytic turnover. MCD and EPR spectra obtained for the H759G MetH mutant reveal that the axial coordination environments of the Co^{2+}Cbl cofactor are also strikingly different in these two protein conformations. Moreover, only the H759G mutant species in the reactivation conformation can be reductively methylated, and the resulting MeCbl species possesses a unique, five-coordinate ligand environment. The implications of these results with respect to the solvent accessibility of the active site in both protein conformations and the possible role of the His759 residue of wild-type MetH in triggering a change between the reactivation conformation and the catalytic conformations are explored.

MATERIALS AND METHODS

Reagents. Methyl viologen, AdoMet, sodium cyanide, guanidine hydrochloride, hydroxocobalamin, MeCbl, trypsin, hydrochloric acid, 37% (HCl), tosyl lysyl chloromethyl ketone (TLCK), 1,3-dibromopropane, 2,2′-dipyridyl, titanium(III) chloride, and Coomassie Brilliant Blue G were obtained from Sigma-Aldrich and used without further purification. 5-Deazaflavin-3-sulfonate was a gift from the late Professor Vincent Massey (University of Michigan). Triquat (1,1′-trimethylene-2,2′-dipyridinium dibromide) was synthesized as described previously from 1,3-dibromopropane and 2,2′-dipyridyl (*19*). *E. coli* Fld and ferrodoxin (flavodoxin):$NADP^+$ oxidoreductase were purified according to published procedures (*3*, *4*). Titanium(III) citrate was prepared from titanium(III) chloride as described previously (*20*, *21*).

H759G MetH Expression and Purification. A protocol for the expression and purification of the H759G variant of

MetH, isolated with the cofactor in the Co^{2+}Cbl state, has been developed previously and was used here with the following minor modifications (*22*). After purification using DEAE-Sepharose, the enzyme was dialyzed overnight against 10 mM potassium phosphate buffer, pH 7.2, at 4 °C. The protein was then loaded onto a MonoQ 16/10 column on an AKTA FPLC (GE Healthcare) equilibrated with 10 mM potassium phosphate buffer, pH 7.2. The column was washed with 40 mL of 10 mM potassium phosphate buffer at 5 mL/min, and then the protein was eluted with a 240 mL linear gradient from 10 to 330 mM potassium phosphate buffer, pH 7.2. The fractions associated with the two major peaks were pooled separately and dialyzed overnight against 10 mM potassium phosphate buffer, pH 7.2, at 4 °C. Each of the pooled fractions was further purified by again loading onto a MonoQ 16/10 FPLC column equilibrated with 110 mM potassium phosphate buffer, pH 7.2. The column was washed with 40 mL of the same buffer at 5 mL/min, and the protein was eluted with a 500 mL linear gradient from 110 to 330 mM potassium phosphate buffer, pH 7.2. The fractions were pooled on the basis of their Abs spectra, concentrated, and then exchanged into 10 mM potassium phosphate buffer, pH 7.2, for storage at −80 °C.

Partial Proteolysis of H759G MetH. The two different forms of Co^{2+}Cbl-bound H759G MetH were cleaved by partial proteolysis as described previously with the following minor modifications (*2*, *13*). Trypsin (3% w/w) was added to the enzyme (3.6 μM in 12 mL of 50 mM Tris, pH 7.2) to initiate proteolysis. The reaction was allowed to proceed for 30 min at room temperature before it was quenched with TLCK (0.015 mg/mL final concentration). The solution was concentrated to 2 mL and the buffer exchanged with 25 mM potassium phosphate buffer, pH 7.2, in an Amicon Ultra-15 concentrator at 4 °C. The solution was loaded onto a MonoQ HR 5/5 column on an AKTA FPLC that was equilibrated with 25 mM potassium phosphate buffer, pH 7.2. The column was washed at 1 mL/min with 20 mL of 25 mM potassium phosphate buffer, pH 7.2. The fragments were then eluted with a 25 mL linear gradient from 25 to 260 mM potassium phosphate buffer, pH 7.2, while collecting 0.5 mL fractions. The fractions were analyzed by SDS−PAGE on 12% acrylamide gels and visualized by staining with Coomassie Brilliant Blue G.

Determination of Cbl Extinction Coefficients and Concentrations When Bound to H759G MetH. Denaturing MetH in guanidine hydrochloride releases Cbl; hence, by collecting the Abs spectrum of the liberated cofactor and using published molar extinction coefficients, the concentration of the protein solution can be readily established. This approach also allows for a straightforward determination of the extinction coefficients of the enzyme-bound cofactor species, as demonstrated previously for the MeCbl-bound state of wild-type MetH (*12*). In the present case, this method was used not only for determining extinction coefficients of various forms of the cofactor bound to MetH but also as a means for quantifying the fraction of Co^{2+}Cbl-bound H759G MetH that was converted to MeCbl-containing protein via electrochemical or enzymatic methylation. As a mixture of different Cbl forms (aquocobalamin, Co^{2+}Cbl, and MeCbl) was typically released from the protein in these experiments, the relative concentrations had to be determined via spectral deconvolution, which was complicated by the fact that the corresponding Abs spectra are strikingly similar. Therefore, sodium cyanide was added to convert the Co^{2+}Cbl and aquocobalamin released from the protein to dicyanocobalamin, as described below. The spectrum of this form of the cofactor could be easily distinguished from that of MeCbl, which does not react with cyanide (*23*, *24*).

In a typical experiment, a stock solution of the enzyme (∼100 μM in 10 mM potassium phosphate buffer, pH 7.2) was diluted 5-fold in guanidine hydrochloride (6 M in 80 mM Tris, pH 8.0) containing 2 mM sodium cyanide at 37 °C. The corresponding Abs spectrum was then recorded and compared to the reference spectra of dicyanocobalamin and MeCbl in the same guanidine hydrochloride/sodium cyanide solution. Varying amounts of the reference spectra were combined to produce a trace that best reproduced the experimental Abs spectrum of the released cofactor mixture. This fitting procedure was used to determine both the initial enzyme concentration in order to calculate the extinction coefficient of the bound cofactor and the fraction of MeCbl-containing enzyme after a methylation reaction.

Reduction, Methylation, and Photolysis of Cbl Bound to H759G MetH. H759G MetH is isolated in the Co^{2+}Cbl-bound state (*22*). To convert it to the MeCbl-bound state, the as-isolated enzyme was reductively methylated by AdoMet in an electrochemical cell (*21*). A 1.5−2 mL solution of 50−200 μM enzyme, 500 μM AdoMet, and 500 μM methyl viologen in buffer (0.1 M potassium phosphate buffer, pH 7.2, with 0.2 M KCl) was equilibrated with Ar(g) in an electrochemical cell with a gold working electrode (*25*). The cell was poised at −450 mV vs SHE at room temperature for 1−2 h. Following methylation in the electrochemical cell, the sample was subjected to chromatography in order to separate residual Co^{2+}Cbl-bound enzyme from MeCbl-containing enzyme. The protein was purified by gel filtration using Sephadex G-50 (Amersham Biosciences), equilibrated with 0.1 M potassium phosphate buffer, pH 7.2, and then loaded onto a MonoQ 16/10 FPLC column equilibrated with 110 mM potassium phosphate buffer, pH 7.2. The column was washed with 40 mL of the same buffer at 5 mL/min, and the protein was eluted with a 500 mL linear gradient from 110 to 330 mM potassium phosphate buffer, pH 7.2. The fractions were pooled on the basis of their Abs spectra, concentrated, and then exchanged into 10 mM potassium phosphate buffer, pH 7.2. In a different set of methylation experiments, triquat was used in place of methyl viologen, and the cell was poised at −600 mV vs SHE for up to 5 h.

The Co^{2+}Cbl-bound state of MetH can also be reductively methylated using an enzymatic method, i.e., by employing the in vivo methylating system consisting of Fld, ferrodoxin (flavodoxin):$NADP^+$ oxidoreductase, and NADPH. Following a procedure published previously (*21*), a 1 mL solution of 10−100 μM enzyme, 500 μM AdoMet, 2.5 μM flavodoxin, and 1 mM NADPH in buffer (100 mM potassium phosphate, pH 7.2) was placed in an anaerobic glass cuvette with a side arm containing ferrodoxin (flavodoxin):$NADP^+$ oxidoreductase (2.5 μM final concentration after mixing). The solution was equilibrated with Ar(g), and the methylation reaction was started by adding the contents of the side arm

to the MetH solution. The progress of the reaction was monitored spectrophotometrically at 450 nm for 90 min.

In some experiments MeCbl-containing MetH was converted back to the Co^{2+}Cbl-bound state by photolysis as follows. An enzyme solution (10−50 μM in 100 mM potassium phosphate buffer, pH 7.2) in an anaerobic cuvette was equilibrated with Ar(g). The cuvette was placed in a large beaker filled with ice water and irradiated repeatedly with a 600 W tungsten/halogen lamp for 10 s. An Abs spectrum was recorded after each irradiation until no further spectral changes were observed.

The Co^{1+}Cbl-bound state of MetH was generated by chemical reduction of the as-isolated enzyme with titanium(III) citrate (*21*). A 1 mL solution of 10−50 μM enzyme in 100 mM potassium phosphate buffer, pH 7.2, was equilibrated with Ar(g) in an anaerobic glass cuvette with a septum and a screw cap. Titanium(III) citrate (250−500 μM final concentration) was added via a syringe through the septum.

The Co^{2+}Cbl-bound state of MetH was also subjected to temperature-dependent spectroscopic experiments as well as a titration with AdoMet. For these experiments, MetH (10 μM in 100 mM potassium phosphate buffer, pH 7.2) was placed in the sample cuvette, and an equal amount of buffer was placed in the reference cuvette of a Cary Bio 300 double-beam UV−vis spectrophotometer. In the temperature-dependent experiments, the samples were allowed to equilibrate for 2 min after the desired temperature was reached before a spectrum was recorded. In the AdoMet titration experiment, equal volumes of a 38 mM stock solution of AdoMet were added to both cuvettes and gently mixed with a stir bar at 37 °C. Again, the contents were allowed to equilibrate for 2 min prior to recording spectra.

Spectrophotometric Determination of the Co^{2+}Cbl/Co^{1+}Cbl Midpoint Potential of H759G MetH. The midpoint potential was measured as described previously (*26*). Briefly, a 1 mL solution of 35 μM enzyme, 100 μM methyl viologen, and 5 μM 5-deazaflavin-3-sulfonate in buffer (100 mM potassium phosphate, 100 mM KCl, and 25 mM EDTA, pH 7.2) was equilibrated with Ar(g) in an anaerobic glass cuvette. The enzyme was reduced by irradiation with a 600 W tungsten/halogen lamp, and the slow oxidation at 37 °C was monitored by Abs spectroscopy. The concentration of reduced methyl viologen was calculated on the basis of the absorbance at 600 nm (ϵ_{600} = 13600 M^{-1} cm^{-1}) (*27*), taking into account that the enzyme also weakly absorbs at this wavelength. These values were used in the Nernst equation, along with the midpoint potential for methyl viologen (−446 mV vs SHE), to calculate the system potential at each time point. Then, the absorbance at 468 nm was corrected for contributions from methyl viologen and used to calculate the concentrations of Co^{2+}Cbl [ϵ_{468} = 10940 M^{-1} cm^{-1} (FPLC fraction 1), ϵ_{468} = 11740 M^{-1} cm^{-1} (FPLC fraction 2)] and Co^{1+}Cbl enzyme [ϵ_{468} = 2000 M^{-1} cm^{-1} (FPLC fraction 2)]. The midpoint potential was then determined graphically from a Nernst plot of the cell potential vs log [Co^{2+}Cbl/Co^{1+}Cbl].

Spectroscopic Experiments. Low-temperature Abs and MCD spectra were obtained using a Jasco J-715 spectropolarimeter in conjunction with an Oxford Instruments SM4000-8T magnetocryostat. For these experiments, the two FPLC fractions containing the different forms of Co^{2+}Cbl-bound H759G MetH, stored at −80 °C in 10 mM potassium phosphate buffer, were thawed on ice and mixed with glycerol (60% v/v) to ensure glass formation at low temperature. Each fraction was then loaded into an MCD sample cell and immediately frozen in liquid N_2. All sample preparation steps took place under an atmosphere of N_2(g) to prevent oxidation to the cob(III)alamin state. The final concentration of Co^{2+}Cbl in each sample, which ranged from 230 to 250 μM, was determined spectrophotometrically at room temperature with a Varian Cary 5e spectrophotometer [ϵ_{468} = 10940 M^{-1} cm^{-1} (FPLC fraction 1), ϵ_{468} = 11740 M^{-1} cm^{-1} (FPLC fraction 2)].

Samples of base-on MeCbl and base-off MeCbl were prepared in 10 mM potassium phosphate buffer (pH 7.2) and 0.1 M aqueous HCl (pH 1.0), respectively. MeCbl-bound H759G MetH [H759G(met)], stored at −80 °C in 10 mM potassium phosphate buffer, pH 7.2, was thawed on ice. After the addition of glycerol (60% v/v), each sample was loaded into an MCD sample cell and immediately frozen in liquid N_2. All sample preparation steps were carried out under minimal ambient light to prevent photolytic cleavage of the Co−C bond. Abs and MCD spectra on fluid solutions of the MeCbl-containing samples were obtained at 280 K, under an atmosphere of He(g), using the same instrumentation as described above for the 4.5 K experiments. The final concentration of MeCbl in each sample, which ranged from 290 to 650 μM, was determined spectrophotometrically at 280 K using published molar extinction coefficients (*12*).

A Bruker ESP 300E spectrometer equipped with a Varian EIP model 625A CW frequency counter, along with an Oxford Instruments ESR 900 continuous flow liquid helium cryostat regulated by an Oxford ITC4 temperature controller, was used to obtain X-band EPR spectra. All spectra were collected with 2 mW of microwave power using a field modulation of 5 G and 100 kHz and a time constant of 300 ms. EPR samples of the Co^{2+}Cbl-bound H759G MetH fractions were prepared anaerobically as described above for the MCD experiments except that in this case the Co^{2+}Cbl concentration was ∼200 μM and the glycerol content varied between 30% and 60% (v/v). After degassing on a vacuum line and purging with Ar(g), each sample was loaded into a quartz EPR tube under Ar(g) and immediately frozen in liquid N_2. EPR spectral simulations were performed using the SIMPOW6 program, developed by Dr. Mark Nilges at the University of Illinois based on the QPOW program (*28*), and assuming collinear **g** and **A** tensors. The complete parameter sets for the EPR simulations are included in the Supporting Information.

RESULTS AND ANALYSIS

Two Fractions Are Isolated during the Purification of Co^{2+}Cbl-Bound H759G MetH. During the purification of as-isolated (i.e., Co^{2+}Cbl-bound) H759G MetH, two major peaks of approximately equal intensity were observed in the FPLC trace (Figure 3). The fractions associated with peak 1 and peak 2 were pooled separately, and their Abs spectra were recorded. While these Abs spectra confirmed that both fractions contained Co^{2+}Cbl-bound MetH, they also revealed slight differences between the two fractions that, together with their different elution times on the MonoQ column, prompted further investigation. A second FPLC step was therefore added to the purification procedure with a more

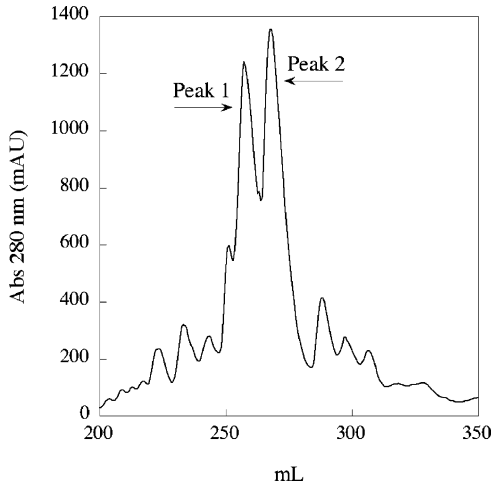

FIGURE 3: FPLC trace of Co^{2+}Cbl-bound H759G MetH obtained using a MonoQ 16/10 column. The two fractions labeled peak 1 and peak 2 correspond to H759G(cat) and H759G(act), respectively.

shallow gradient to more completely separate the MetH fractions associated with the two peaks. The two fractions were then subjected to proteolysis and electrophoresis to determine the specific protein conformation in each case.

The Two Fractions of Co^{2+}Cbl-Bound H759G MetH Are in Different Conformations. On limited proteolysis with trypsin, the two fractions of Co^{2+}Cbl-bound H759G MetH display the same cleavage pattern. Specifically, in each case the enzyme was cleaved into three major fragments, as previously reported: the Cbl-containing module (28 kDa), the AdoMet-binding module (38 kDa), and the combined Hcy- and CH_3-H_4folate-binding modules (70 kDa) (*11*). However, when the cleaved enzyme was loaded onto a MonoQ FPLC column after proteolysis, a significant difference was noted in the pattern of elution of the fragments (Figure 4). While the Cbl-containing module eluted together with the combined Hcy- and CH_3-H_4folate-binding modules when the fraction associated with peak 1 was cleaved, it eluted with the AdoMet-binding module upon proteolysis of the fraction associated with peak 2. In each case the fragments were completely cleaved, as revealed by gel electrophoresis, yet they eluted together, suggesting noncovalent interactions between them that likely already existed before cleavage. Collectively, these observations suggest that the two forms of Co^{2+}Cbl-bound H759G MetH differ with respect to the specific enzyme conformation; i.e., in fraction 1, the dominant interaction involves the Cbl-binding and catalytic substrate-binding modules (conformations used in the catalytic cycle), while in fraction 2, the dominant interaction appears to occur between the Cbl-binding and AdoMet-binding modules (corresponding to the conformation used in the reactivation cycle). Therefore, fractions 1 and 2 of the Co^{2+}Cbl-bound H759G MetH mutant are hereafter referred to as H759G(cat) and H759G(act), respectively, based upon the predominant protein conformation in each fraction.

Abs and MCD Spectroscopic Studies of Co^{2+}Cbl-Bound H759G MetH. The peak positions of the dominant features in the visible region of the Abs spectrum of the two distinct fractions of Co^{2+}Cbl-bound H759G MetH (Figure 5) are very similar [bands at 21280 and 21390 cm^{-1} for H759G(act) and H759G(cat), respectively, at 4.5 K]. On the basis of the peak

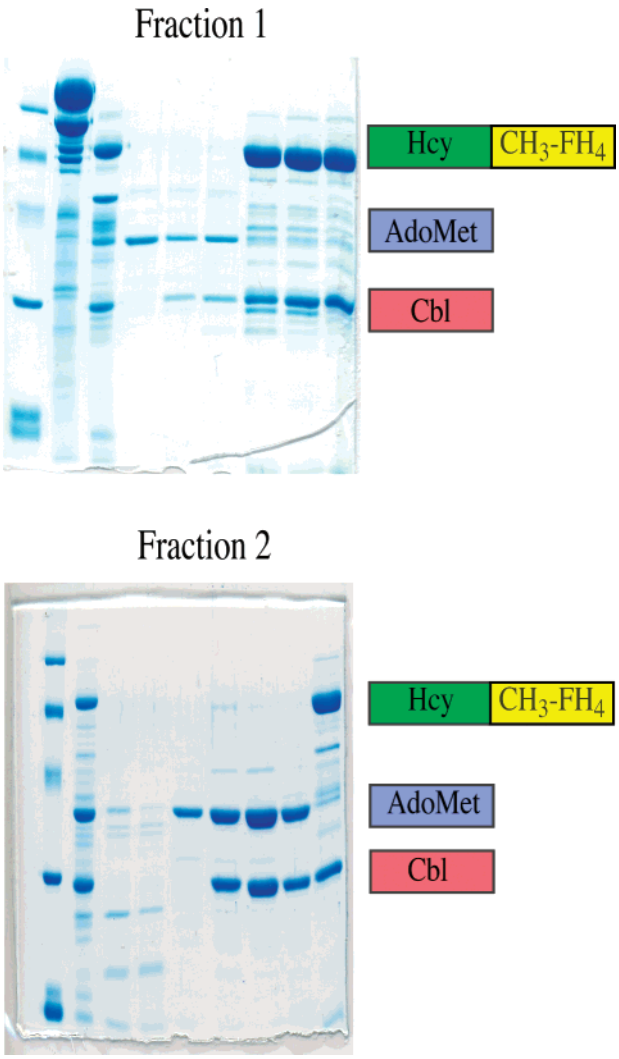

FIGURE 4: SDS−PAGE gels of the products obtained by partial proteolysis of the two distinct FPLC fractions of Co^{2+}Cbl-bound H759G MetH. In each case the enzyme was cleaved into three major fragments: the Cbl-binding module (28 kDa, red), the AdoMet-binding module (38 kDa, blue), and the combined Hcy- and CH_3-H_4folate-binding modules (70 kDa, green and yellow). However, while in the case of fraction 1 (top panel) the fragments corresponding to the Cbl-binding module and the combined Hcy- and CH_3-H_4folate-binding modules eluted together, the Cbl- and AdoMet-binding modules eluted together when fraction 2 was used (bottom panel).

positions reported for aqueous Co^{2+}Cbl (21230 cm^{-1}) and cob(II)inamide (Co^{2+}Cbi$^+$, 21280 cm^{-1}) (*17*), the latter of which serves a model of base-off Co^{2+}Cbl (Co^{2+}Cbi$^+$ lacks the nucleotide loop and dimethylbenzimidazole and thus binds a water molecule in the axial position), this result suggests a base-off coordination environment for the Co^{2+}-Cbl cofactor in both fractions of Co^{2+}Cbl-bound H759G MetH. In addition to the slight blue shift of the dominant visible Abs feature from H759G(act) to H759G(cat), noticeable differences also exist in the overall shape of the Abs envelope. This suggests that a more dramatic difference in the electronic structure of the Co^{2+}Cbl cofactor in H759G-(act) and H759G(cat) is potentially masked in the Abs spectra where the individual electronic transitions combine to produce a single dominant feature in the visible region.

Compared to Abs spectroscopy, MCD spectroscopy offers a far more sensitive probe of the electronic structure of Co^{2+}-

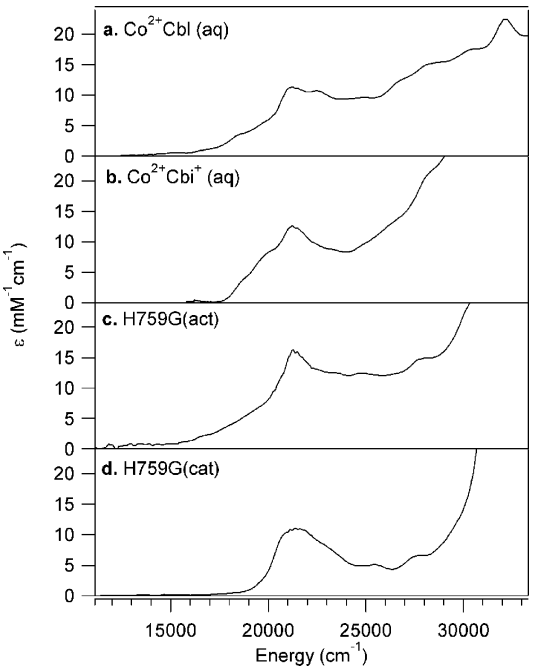

FIGURE 5: 4.5 K Abs spectra of (a) aqueous Co^{2+}Cbl, (b) aqueous $Co^{2+}Cbi^{+}$, (c) Co^{2+}Cbl-bound H759G MetH(act), and (d) Co^{2+}-Cbl-bound H759G MetH(cat).

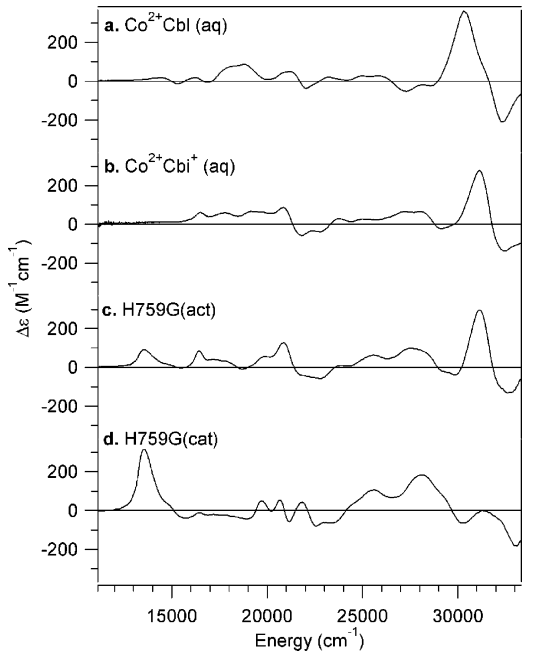

FIGURE 6: 7T, 4.5 K MCD spectra of (a) aqueous Co^{2+}Cbl, (b) aqueous $Co^{2+}Cbi^{+}$, (c) Co^{2+}Cbl bound to H759G MetH(act), and (d) Co^{2+}Cbl bound to H759G MetH(cat).

Cbl due to the increased band resolution inherent to a signed spectrum and the dramatic increase in the relative intensities of electronic transitions involving MOs with predominant Co 3d orbital character. Indeed, a comparison of the MCD spectra of the aqueous Co^{2+}Cbl and $Co^{2+}Cbi^{+}$ cofactors and the two distinct fractions of Co^{2+}Cbl-bound H759G MetH reveals significant differences in the spectral region below 22000 cm^{-1} (Figure 6). This region of the Co^{2+}Cbl MCD spectrum has previously been shown to be dominated by electronic transitions that are primarily Co d → d in character (*17*). These Co d → d transitions are particularly sensitive to the nature of the axial ligand, as evidenced by the significant differences between the MCD spectra of aqueous Co^{2+}Cbl and $Co^{2+}Cbi^{+}$ (Figure 6, traces a and b). Overall, the H759G(act) MCD spectrum is qualitatively similar to that of aqueous $Co^{2+}Cbi^{+}$; hence, the Co^{2+}Cbl species in the H759G(act) fraction can be described as being five-coordinate with an axially bound water ligand (Figure 6, traces b and c).[2] In contrast, since H759G(cat) exhibits an MCD feature at ~13500 cm^{-1} that is absent in the spectra of aqueous Co^{2+}Cbl and $Co^{2+}Cbi^{+}$ (Figure 6, trace d), it must contain a Co^{2+}Cbl species that possesses a unique axial coordination environment.

Insight into the nature of the unique axial Co^{2+} coordination environment of the Co^{2+}Cbl species in H759G(cat) can be obtained from a qualitative analysis of the spectral features associated with the Co d → d transitions. A combined spectroscopic and density functional theory (DFT) computational study of the Co^{2+}Cbl and $Co^{2+}Cbi^{+}$ cofactors in aqueous solution has revealed that the singly occupied molecular orbital (SOMO) of each of these low-spin d^7 electronic systems is derived primarily from the Co $3d_{z^2}$ orbital. The remaining six "d electrons" occupy MOs possessing predominant Co $3d_{yz}$, $3d_{xz}$, and $3d_{x^2-y^2}$ character (*17*). Therefore, ignoring the effects of electron−electron repulsion, the energies of the first few electronic transitions in Co^{2+}corrinoid species should roughly correspond to the energy differences between the fully occupied Co 3d-derived MOs and the Co $3d_{z^2}$-based SOMO. Because the Co $3d_{z^2}$ orbital is oriented directly toward the axial coordination sites, the energy of the SOMO is considerably more perturbed than those of the remaining Co 3d-based MOs by changes in the axial ligation. Consequently, the significant red shift of the first observed electronic transition from aqueous $Co^{2+}Cbi^{+}$ to H759G(cat) implies that the weakly σ-donating axial water ligand that is present in $Co^{2+}Cbi^{+}$ must partially dissociate from the Co^{2+} center or be replaced by an even more weakly σ-donating ligand to generate an effectively four-coordinate Co^{2+}Cbl species in H759G(cat) (Figure 6, traces b and d). A similar MCD spectral perturbation has previously been observed for two adenosyltransferases, where it was ascribed to the conversion of five-coordinate Co^{2+}Cbl to a putative four-coordinate species (*29*, *30*).

EPR Spectroscopic Data. The X-band EPR spectra of aqueous Co^{2+}Cbl and $Co^{2+}Cbi^{+}$ reveal that the *g* values and metal hyperfine parameters [*A*(Co)] are extremely sensitive to the axial ligation of the Co^{2+} center (Figure 7). Specifically, the increase in g_1 and g_2 from Co^{2+}Cbl to $Co^{2+}Cbi^{+}$ can be attributed to a decrease in the energy difference between the Co $3d_{z^2}$-based SOMO and the doubly occupied Co $3d_{yz}$- and $3d_{xz}$-based MOs with a weakening of the Co-axial ligand bonding interaction, which simultaneously also leads to an increase in *A*(Co) (*17*). Additionally, the ^{14}N superhyperfine splittings evident in the g_3 region of the Co^{2+}-Cbl EPR spectrum vanish upon replacement of the axial nitrogen donor ligand 5,6-dimethylbenzimidazole with a

[2] The feature at ~13500 cm^{-1} in the H759G(act) MCD spectrum, which has no counterpart in the $Co^{2+}Cbi^{+}$ spectrum, is attributed to a minor contribution from H759G(cat). Although apparent base-line separation has been achieved using FPLC, as judged by the homogeneity of the samples taken across each peak, there is a small amount of cross-contamination of each fraction as judged on the basis of our MCD and EPR data (Figures S1 and S2, Supporting Information).

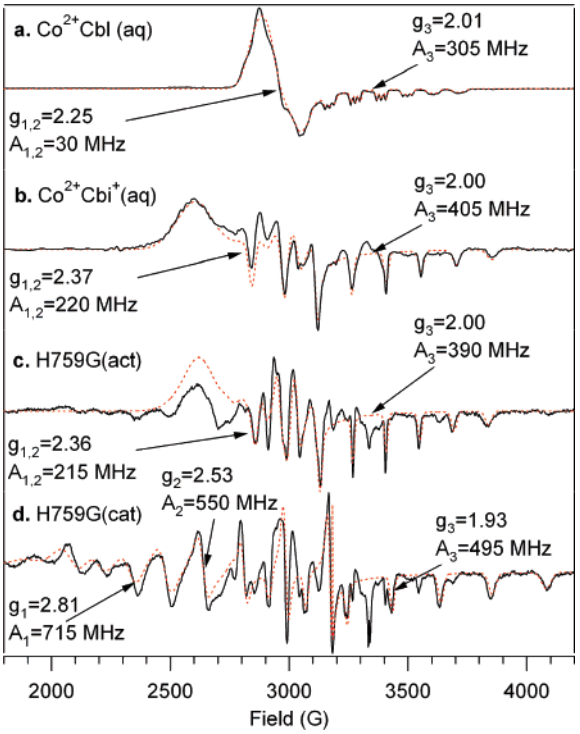

FIGURE 7: Experimental (solid line) and simulated (dotted line) X-band (9.35 GHz) EPR spectra of (a) aqueous Co^{2+}Cbl, (b) aqueous $Co^{2+}Cbi^{+}$, (c) Co^{2+}Cbl bound to H759G MetH(act), and (d) Co^{2+}Cbl bound to H759G MetH(cat). Note that the EPR spectrum of aqueous Co^{2+}Cbl was simulated with an isotropic A(N) coupling of 55 MHz to account for the additional fine structure. Complete parameter sets are available in Tables S1−S4.

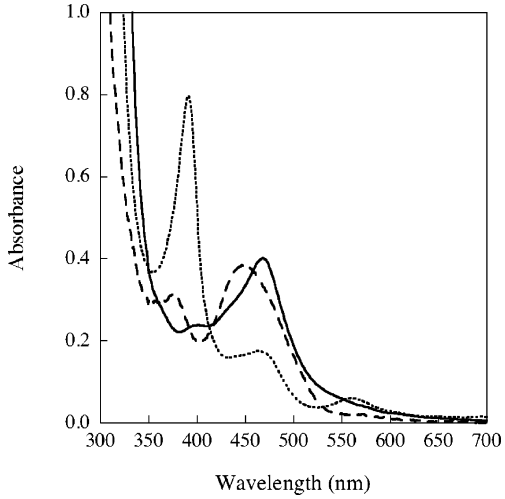

FIGURE 8: Abs spectra of different forms of H759G MetH. When the as-isolated (i.e., Co^{2+}Cbl-bound) H759G(act) form (solid trace) was reduced with titanium citrate, a Co^{1+}Cbl-bound species (dotted trace) was obtained. Alternatively, when Co^{2+}Cbl-bound H759G-(act) was subjected to electrochemical methylation with AdoMet, a MeCbl-bound species was obtained (dashed trace). All spectra were obtained in 50 mM potassium phosphate buffer, pH 7.2, at 37 °C.

water molecule as in aqueous $Co^{2+}Cbi^{+}$. For the H759G-(act) fraction, the g and A(Co) values extracted from the X-band EPR spectrum are very similar to those obtained for aqueous $Co^{2+}Cbi^{+}$, indicating that in the reactivation conformation the Co^{2+}Cbl cofactor favors a five-coordinate ligand environmentwith a water molecule in the axial position, consistent with our MCD data discussed above.[3]

A qualitative analysis of the H759G(cat) EPR data (Figure 7) also fully supports the conclusions drawn from the corresponding MCD data. In particular, our hypothesis that in the catalytic cycle conformation the Co^{2+}Cbl cofactor possesses a unique axial ligand environment is entirely consistent with the fact that the corresponding g_1, g_2, and A(Co) values are significantly larger than those observed for either Co^{2+}Cbl or $Co^{2+}Cbi^{+}$ in aqueous solution.[4] In analogy to the red shift of the first observed electronic transition, the dramatic increase in g_1 and g_2 from aqueous $Co^{2+}Cbi^{+}$ to H759G(cat) can also be rationalized in terms of (partial) axial ligand dissociation and the consequent decrease in energy splitting between the Co 3d-based SOMO and the occupied Co 3d-derived MOs. Specifically, this reduction in Co 3d orbital splitting from aqueous $Co^{2+}Cbi^{+}$ to H759G-(cat) causes an increase in spin−orbit mixing of ligand-field excited-state character into the ground state and, thus, an increase in g_1 and g_2. The presence of an effectively four-coordinate Co^{2+}Cbl species in H759G(cat) is further corroborated by the dramatic increase in the A(Co) values from aqueous $Co^{2+}Cbi^{+}$ to H759G(cat), since the loss of axial ligation necessarily leads to an increase in the unpaired spin density on the Co^{2+} center. Therefore, our EPR data also strongly support the assignment of the unique Co^{2+}Cbl species in the H759G(cat) fraction as an effectively four-coordinate Co^{2+}Cbl species.

Reductive Methylation of the H759G(cat) and H759G-(act) Fractions. In attempts to reductively methylate Co^{2+}-Cbl-bound H759G MetH with AdoMet, only about half of the protein was actually being converted to the MeCbl-bound form H759G(met). On the basis of the MCD spectrum of the corresponding products (Figure S3), the unreacted Co^{2+}-Cbl-bound H759G MetH fraction was almost exclusively H759G(cat). To explore the origin of this puzzling result, each of the two fractions of as-isolated (i.e., Co^{2+}Cbl-bound) H759G MetH was subjected to a separate electrochemical methylation experiment. When the H759G(act) fraction was reductively methylated with AdoMet in the presence of methyl viologen in an electrochemical cell poised at −450 mV vs SHE, almost complete conversion to H759G(met) was accomplished, as revealed by the blue shift of λ_{max} from 468 to 450 nm (Figure 8). However, when the same experiment was carried out with the H759G(cat) fraction, no spectral changes were observed, indicating that in this case methylation of the corresponding Co^{2+}Cbl species did not occur. Even when the reaction was repeated with triquat ($E^{\circ\prime} = -540$ mV) instead of methyl viologen ($E^{\circ\prime} = -446$ mV) and the cell was poised at −600 mV for up to 5 h, no methylation was observed. Additionally, the H759G(cat) fraction could not be converted to the MeCbl form with the in vivo methylation system consisting of Fld, ferrodoxin (flavodoxin):$NADP^{+}$ oxidoreductase, and NADPH, conditions under which the H759G(act) fraction was fully methylated.

A key step in the conversion of MetH-bound Co^{2+}Cbl to MeCbl is the generation of the Co^{1+}Cbl intermediate. Therefore, we sought to measure the reduction midpoint potentials of the Co^{2+}Cbl species in both the H759G(cat)

[3] Also consistent with our MCD data is the presence of an additional weak signal in the low-field region of the H759G(act) EPR spectrum due to the minor contribution from H759G(cat).

[4] Similar to the case of H759G(act) discussed above, a small component of H759G(act) contributes to the H759G(cat) EPR spectrum.

and H759G(act) fractions. H759G(act) was photoreduced to the Co^{1+}Cbl form with 5-deazaflavin-3-sulfonate in the presence of the indicator dye methyl viologen, as indicated by a decrease in absorbance at 468 nm. The reoxidation to the Co^{2+}Cbl form was monitored as an increase in absorbance at 468 nm (Figure 9A). From a Nernst plot, the Co^{2+}-Cbl/Co^{1+}Cbl midpoint potential was calculated to be −490 mV at pH 7.2 (Figure 9B). This value is essentially identical to that reported for wild-type MetH (−490 mV at pH 7.0) and is consistent with the successful methylation of the H759G(act) fraction under reducing conditions (*31*).

In contrast, the H759G(cat) fraction could not be reduced by following the procedure described above for the H759G-(act) fraction (Figure 9C). Moreover, attempts to reduce H759G(cat) using methyl viologen or triquat as mediators were similarly unsuccessful. Hence, the fact that H759G-(cat) cannot be converted to the MeCbl-bound state by electrochemical methylation can be ascribed to the inability of this protein fraction to access the Co^{1+}Cbl state. It should be noted, however, that even if the Co^{1+}Cbl state could be accessed, methylation of H759G(cat) would presumably still not occur because this fraction is trapped in a conformation in which Cbl does not have access to AdoMet (vide supra).

Co^{2+}Cbl-Bound H759G MetH Cannot Switch between the Reactivation and Catalytic Conformations. Once separated by FPLC, the H759G(cat) and H759G(act) fractions remained distinct over time, and any efforts to promote interconversion were unsuccessful. Specifically, when H759G(act) was converted to the MeCbl form and subsequently subjected to photoirradiation, Co^{2+}Cbl-bound H759G(act) was regenerated. Likewise, when H759G(act) was converted to the Co^{1+}-Cbl form, it slowly reoxidized to Co^{2+}Cbl-bound H759G-(act). Finally, neither H759G(cat) nor H759G(act) displayed any Abs spectral changes when the temperature was varied between 10 and 40 °C or upon titration with AdoMet at 37 °C (Figures S4 and S5), indicating that conversion to another conformation did not occur.

Abs and MCD Spectroscopic Studies of MeCbl-Bound H759G MetH. The peak position of the so-called "α-band" in the 280 K Abs spectrum of H759G(met) (22400 cm^{-1}) is significantly blue shifted from those of both base-on MeCbl (19100 cm^{-1}) and base-off MeCbl (21600 cm^{-1}) in aqueous solution (Figure 10). However, except for this difference in the α-band position, the Abs spectra of H759G(met) and base-off MeCbl are very similar, suggesting that the protein-bound cofactor is also in the base-off conformation.

A more sensitive probe of the axial ligand environment of the Co^{3+} center in H759G(met) is provided by MCD spectroscopy. Notably, our MCD data indicate that the first observed electronic transition is in fact even more dramatically blue shifted than suggested by the α-band peak position in the corresponding Abs spectra, shifting from 18200 cm^{-1} for base-on MeCbl to 19200 cm^{-1} for base-off MeCbl to 21000 cm^{-1} for H759G(met) (Figure 11). This transition has previously been assigned as a corrin-centered $\pi \rightarrow \pi^*$ excitation, corresponding to the HOMO → LUMO transition in base-on MeCbl (*16*). Our MCD data therefore reveal that the energy splitting between these corrin π- and π^*-based MOs is significantly larger in H759G(met) than in both base-on and base-off MeCbl. Such an increase in energy splitting could result from a stabilization of the HOMO [or the analogous corrin π-based MO in H759G(met)], a destabilization of the LUMO, or a combination thereof.

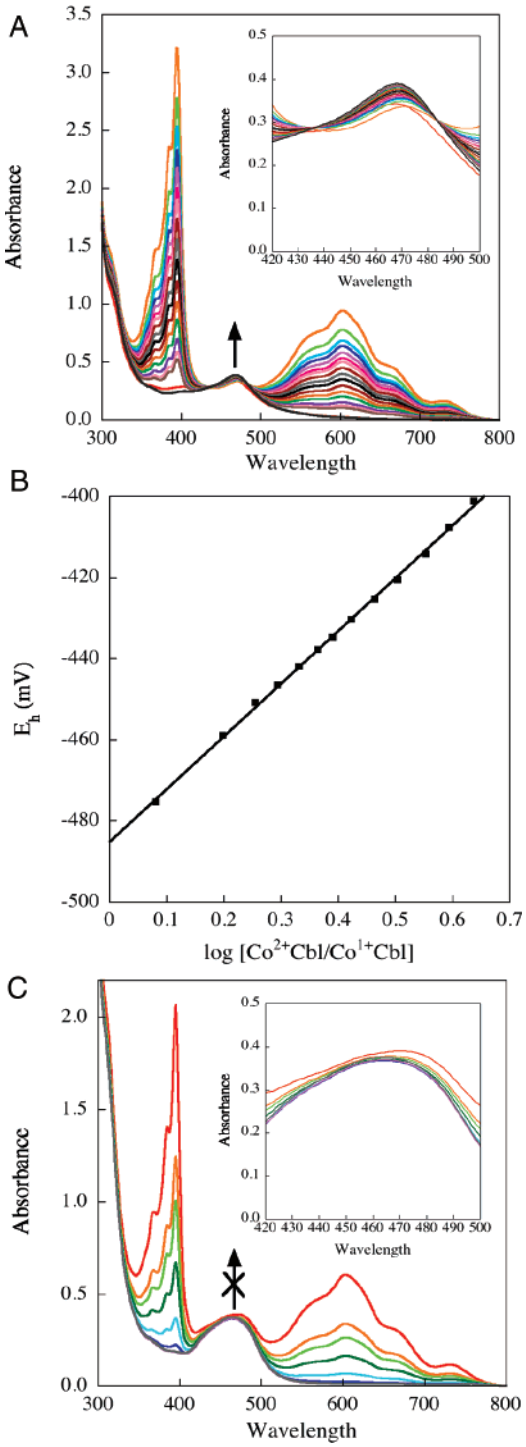

FIGURE 9: Spectrophotometric determination of the Co^{2+}Cbl/Co^{1+}-Cbl midpoint potential of H759G MetH. (A) H759G(act) was first photoreduced with 5-deazaflavin-3-sulfonate in the presence of the indicator dye methyl viologen to generate a Co^{1+}Cbl-bound species (as evidenced by the decrease in absorbance at 468 nm), and spectra were then recorded to monitor the increase in absorbance at 468 nm associated with the spontaneous reoxidation to the Co^{2+}Cbl-bound H759G(act) form. (B) Nernst plot for the Co^{2+}Cbl/Co^{1+}Cbl reduction of H759G(act). From this plot, the midpoint potential was estimated to be −490 mV. (C) Attempts to photoreduce H759G(cat) with 5-deazaflavin-3-sulfonate in the presence of methyl viologen were unsuccessful, as evidenced by the lack of a change in absorbance at 468 nm right after photoreduction and over time as the indicator dye methyl viologen oxidized.

A combined spectroscopic and DFT computational study of MeCbl revealed that the formally unoccupied Co $3d_{z^2}$ orbital is a minor contributor to the corrin π-based HOMO

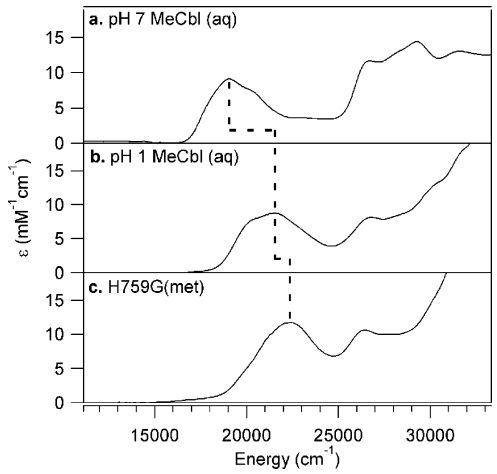

FIGURE 10: 280 K Abs spectra of (a) aqueous, base-on MeCbl, (b) aqueous, base-off MeCbl, and (c) H759G MetH(met). The vertical line serves to illustrate the successive blue shift of the α-band from panels a through c.

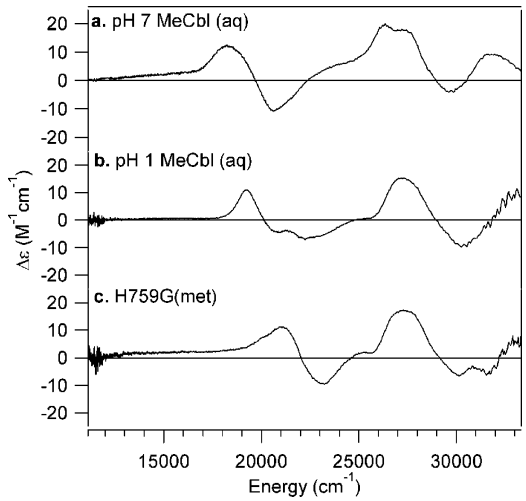

FIGURE 11: 7T, 280 K MCD spectra of (a) aqueous, base-on MeCbl, (b) aqueous, base-off MeCbl, and (c) H759G MetH(met).

(i.e., the donor orbital in the α-band transition) (*16*). This mixing between the corrin π and Co $3d_{z^2}$ orbitals provides a mechanism by which the axial ligand switch from base-on to base-off MeCbl can perturb the energies of the corrin π-based MOs. Since the Co $3d_{z^2}$ orbital is oriented directly toward the axial coordination sites, the energy of this orbital, and thus the corrin π-based HOMO, depends on the σ-donor strength of the axial ligands. As the σ-donor strength of the lower axial ligand trans to the methyl group decreases, the σ-antibonding interaction with the Co $3d_{z^2}$ orbital decreases, giving rise to a stabilization of the HOMO (or the analogous corrin π-based MO) and thus a blue shift of the α-band transition. This prediction is supported by a recent DFT computational study of methylcobinamide ($MeCbi^+$), which demonstrated that a lengthening of the Co−OH_2 bond so as to mitigate the σ-antibonding interaction with the Co $3d_{z^2}$ orbital leads to a stabilization of all MOs possessing significant Co $3d_{z^2}$ character, including the HOMO. According to this study, the α-band is expected to blue shift by ∼20 cm^{-1} per 0.01 Å lengthening of the Co−OH_2 bond (*32*). Thus, the blue shift by 1800 cm^{-1} of the α-band from base-off MeCbl to H759G(met) observed in our MCD data (Figure 10) is consistent with an axial Co−OH_2 bond elongation by at least 0.9 Å. Such a dramatic lengthening of the Co−OH_2 bond in H759G(met) suggests that the axial H_2O ligand may in fact be removed altogether to yield a five-coordinate MeCbl species.

DISCUSSION

Co^{2+}Cbl-Bound H759G MetH Cannot Switch between the Reactivation and Catalytic Conformations. The results obtained in this study reveal that the Co^{2+}Cbl-bound H759G MetH mutant cannot interconvert between the reactivation and catalytic conformations (see Results and Analysis), which parallels the behavior observed for Co^{1+}Cbl-bound wild-type MetH. In the case of wild-type MetH, reduction of the Co^{2+}-Cbl-bound form yields the Co^{1+}Cbl-bound form in the reactivation conformation [Co^{1+}Cbl(act)], whereas demethylation of the MeCbl-bound form by Hcy results in the formation of the Co^{1+}Cbl-bound form in the catalytic conformations [Co^{1+}Cbl(cat)]. Co^{1+}Cbl(act) is selectively methylated by AdoMet, while Co^{1+}Cbl(cat) exclusively utilizes CH_3-H_4folate as the methylating agent (*13*). Furthermore, electron transfer from enzyme-bound Co^{1+}Cbl to oxidized Fld occurs 18000 times faster with Co^{1+}Cbl(act) than Co^{1+}Cbl(cat) (*13*). Collectively, these results indicate that Co^{1+}Cbl(act) and Co^{1+}Cbl(cat) are locked into the reactivation and catalytic protein conformations, respectively, since AdoMet and Fld are known to interact only with Cbl in the reactivation conformation while CH_3-H_4folate interacts exclusively with Cbl in the catalytic conformations (*1*). In contrast, MeCbl-bound and Co^{2+}Cbl-bound wild-type MetH appear to readily undergo transitions between the reactivation and catalytic conformations. Co^{2+}Cbl-bound wild-type MetH assumes the His-off conformation upon the addition of flavodoxin (*10*) and exhibits temperature- and ligand-dependent transitions between the His-on and His-off forms (Fleischhacker and Matthews, manuscript in preparation). The Abs spectrum of MeCbl-bound wild-type MetH exhibits dramatic changes as MetH enters the reactivation conformation and assumes His-off coordination (*11*); this transition is also modulated by temperature and ligands. At present, the molecular basis for this conformational segregation of Co^{1+}Cbl(act) and Co^{1+}Cbl(cat), as well as of H759G(act) and H759G(cat) for any cofactor oxidation state, is unknown. It is interesting to note, however, that all forms of H759G MetH and Co^{1+}Cbl-bound wild-type MetH are always His-off, while MeCbl-bound and Co^{2+}Cbl-bound wild-type MetH are His-on in certain protein conformations. This result suggests that coordination of the His759 residue to the cobalt center may be necessary for the interconversion between the reactivation and catalytic conformations.

The α- ("Lower") and β- ("Upper") Faces of Cbl Are Solvent-Inaccessible in the Catalytic Conformations of H759G MetH. Electrochemical (*15*), X-ray crystallographic (*33*), and electron−nuclear double resonance studies (*34*) have conclusively demonstrated that the Co^{2+} center in base-off Co^{2+}Cbl (and, by analogy, $Co^{2+}Cbi^+$) has a coordination number of five in aqueous solution, possessing a water molecule in one of the axial positions. Hence, the fact that H759G(cat) possesses an effectively four-coordinate Co^{2+}-Cbl species as evidenced by our MCD and EPR data (see Figures 6 and 7) suggests that in the catalytic conformations of MetH the Cbl-binding site is solvent-inaccessible. A solvent-inaccessible Cbl-binding site should minimize unwanted side reactions of both the protein-bound MeCbl and Co^{1+}Cbl species that participate in the catalytic cycle of MetH.

Previous studies revealed that the Cbl-binding domain of MetH features a protein cage that encourages radical

recombination following inadvertent homolytic cleavage of the Co−C bond of the enzyme-bound MeCbl cofactor (*35*). Solvent access would be expected to undermine the effectiveness of this protein cage and thus to shorten the lifetime of the MeCbl-bound resting state of MetH by providing alternative reaction pathways for the transiently formed methyl radical. Additionally, because of its "supernucleophilic" character, the Co^{1+}Cbl species formed during catalytic turnover is poised for nucleophilic attack of a wide range of substrates (*36*, *37*). Solvent access would likely permit the enzyme-bound Co^{1+}Cbl species to attack substrates other than CH_3-H_4folate, thereby precluding the reformation of MetH-bound MeCbl. Recovery of the MetH resting state via the reactivation cycle following both the loss of the methyl radical and the inactivation of the Co^{1+}-Cbl reaction intermediate requires AdoMet, a compound derived from the Met product of MetH (*38*). This makes excessive usage of the reactivation cycle disadvantageous to the cell by depleting the intracellular supply of AdoMet.

Only the β- ("Upper") Face of Cbl Is Solvent-Accessible in the Reactivation Conformation of H759G MetH. Because the MCD and EPR spectra of H759G(act) are very similar to those of aqueous $Co^{2+}Cbi^{+}$ (Figures 6 and 7), it follows that H759G(act) contains a five-coordinate Co^{2+}Cbl species with an axially bound water molecule. While this result indicates that in the reactivation conformation of H759G MetH the Cbl-binding site is solvent-accessible, it is not possible to determine whether the axial water ligand is bound to the α- or β-face of the cofactor on the basis of our spectroscopic data alone. However, considering that the axial oxygen-donor ligands in cob(II)ester, a close mimic of base-off Co^{2+}Cbl, and the Co^{2+}Cbl species in the corrinoid:iron sulfur protein bind to the Co center on the sterically less hindered β-face, as revealed by X-ray crystallographic data (*33*, *39*), it is reasonable to assume that the Co^{2+}Cbl species in H759G(act) also binds its water molecule on the β-face.

Additional indirect support for this proposal is provided by our H759G(met) spectroscopic data. Because photolysis of H759G(met), which is formed by reductive methylation of H759G(act), exclusively produces H759G(act), it can be concluded that H759G(met) is locked into the reactivation conformation of MetH. Hence, the fact that our Abs and MCD spectra reveal that the water molecule that coordinates on the α-face of base-off MeCbl(aq) is no longer present in H759G(met) (Figures 10 and 11) suggests that in the reactivation conformation of MetH the α-face is solvent-inaccessible.

Examination of the X-ray crystal structure of a truncated H759G MetH variant (residues 649−1227), which is forced to adopt the reactivation conformation, also supports the hypothesis that the β-face of the Cbl cofactor in H759G-(cat) is solvent-accessible (Figure 12) (*14*). Hence, in this conformation the Co^{2+} center has much better access to external reductants, such as Fld or mediator dyes (*11*), than in the catalytic conformations, in which the cofactor is solvent-inaccessible (vide supra). Moreover, as suggested by the results obtained in cross-linking experiments with wild-type MetH and Fld as well as the X-ray crystal structure of truncated H759G MetH that is trapped in the reactivation conformation (*3*, *14*), the β-face of the Cbl cofactor may become solvent-inaccessible upon docking of Fld to MetH. Since the axial water molecule in H759G(act) binds exclusively to the β-face of Co^{2+}Cbl, as demonstrated in this study, it may readily dissociate upon Fld docking so as to yield a four-coordinate Co^{2+}Cbl intermediate prior to, or concomitant with, the reduction of Co^{2+}Cbl to Co^{1+}Cbl in the reactivation cycle of MetH. A four-coordinate Co^{2+}Cbl intermediate fits the paradigm of enzymatic Co^{2+}Cbl → Co^{1+}-Cbl reduction first suggested on the basis of spectroscopic studies of two adenosyltransferases (*29*, *30*) and provides an intuitively appealing explanation as to why this step is thermodynamically feasible despite the apparent mismatch of the Co^{2+}Cbl and Fld reduction potentials (*40*).

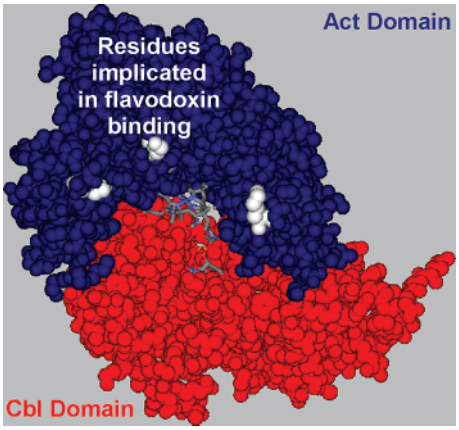

FIGURE 12: Space-filling representation of the X-ray crystal structure of the truncated H759G MetH variant (residues 649−1227) that only contains the Cbl- and AdoMet-binding modules and is thus forced to adopt the same conformation as H759G MetH-(act) (*14*). Residues implicated in Fld docking are highlighted in white (*3*). Note that while the α-face of the Cbl cofactor is protected by the Cbl-binding module (red), the β-face is left partially solvent-accessible by the AdoMet-binding module (blue).

ACKNOWLEDGMENT

We thank Prof. Tim Machonkin and Dr. Troy Stich for useful discussions, especially with respect to the H759G-(cat) EPR spectrum. We also thank Prof. Mark Nilges and the Illinois EPR Research Center for providing us with a copy of the SIMPOW6 program.

SUPPORTING INFORMATION AVAILABLE

Additional Abs and MCD data mentioned, but not discussed in text, as well as complete parameter sets for the SIMPOW6 EPR simulations. This material is available free of charge via the Internet at http://pubs.acs.org.

REFERENCES

1. Goulding, C. W., Postigo, D., and Matthews, R. G. (1997) Cobalamin-Dependent Methionine Synthase Is a Modular Protein with Distinct Regions for Binding Homocysteine, Methyltetrahydrofolate, Cobalamin, and Adenosylmethionine, *Biochemistry 36*, 8082−8091.
2. Drummond, J. T., Huang, S., Blumenthal, R. M., and Matthews, R. G. (1993) Assignment of Enzymatic Function to Specific Protein Regions of Cobalamin-Dependent Methionine Synthase from *Escherichia coli*, *Biochemistry 32*, 9290−9295.
3. Hall, D. A., Jordan-Starck, T. C., Loo, R. O., Ludwig, M. L., and Matthews, R. G. (2000) Interaction of Flavodoxin with Cobalamin-Dependent Methionine Synthase, *Biochemistry 39*, 10711−10719.
4. Hall, D. A., Vander, Kooi, C. W., Stasik, C. N., Stevens, S. Y., and Zuiderweg, E. R. P. (2001) Mapping the Interaction Between Flavodoxin and its Physiological Partners Flavodoxin Reductase and Cobalamin-Dependent Methionine Synthase, *Proc. Natl. Acad. Sci. U.S.A. 98*, 9521−9526.
5. Evans, J. C., Huddler, D. P., Hilgers, M. T., Romanchuk, G., Matthews, R. G., and Ludwig, M. L. (2004) Structures of the

N-terminal Modules Imply Large Domain Motions During Catalysis by Methionine Synthase, *Proc. Natl. Acad. Sci. U.S.A. 101*, 3729−3736.
6. Banerjee, R. V., Frasca, V., Ballou, D. P., and Matthews, R. G. (1990) Participation of Cob(I)alamin in the Reaction Catalyzed by Methionine Synthase from *Escherichia coli*: A Steady-State and Rapid Reaction Kinetic Analysis, *Biochemistry 29*, 11101−11109.
7. Taylor, R. T., and Weissbach, H. (1967) N^5-Methyltetrahydrofolate-Homocysteine Transmethylase, *J. Biol. Chem. 242*, 1502−1508.
8. Fujii, K., and Huennekens, F. M. (1974) Activation of Methionine Synthetase by a Reduced Triphosphopyridine Nucleotide-Dependent Flavoprotein System, *J. Biol. Chem. 249*, 6745−6753.
9. Mangum, J. H., and Scrimgeour, K. G. (1962) Cofactor Requirements and Intermediates in Methionine Biosynthesis, *Fed. Proc. 21*, 242.
10. Hoover, D. M., Jarrett, J. T., Sands, R. H., Dunham, W. R., Ludwig, M. L., and Matthews, R. G. (1997) Interaction of *Escherichia coli* Cobalamin-Dependent Methionine Synthase and its Physiological Partner Flavodoxin: Binding of Flavodoxin Leads to Axial Ligand Dissociation from the Cobalamin Cofactor, *Biochemistry 36*, 127−138.
11. Jarrett, J. T., Hoover, D. M., Ludwig, M. L., and Matthews, R. G. (1998) The Mechanism of Adenosylmethionine-Dependent Activation of Methionine Synthase: A Rapid Kinetic Analysis of Intermediates in Reductive Methylation of Cob(II)alamin Enzyme, *Biochemistry 37*, 12649−12658.
12. Jarrett, J. T., Amaratunga, M., Drennan, C. L., Scholten, J. D., Sands, R. H., Ludwig, M. L., and Matthews, R. G. (1996) Mutations in the B_{12}-Binding Region of Methionine Synthase: How the Protein Controls Methylcobalamin Reactivity, *Biochemistry 35*, 2464−2475.
13. Jarrett, J. T., Huang, S., and Matthews, R. G. (1998) Methionine Synthase Exists in Two Distinct Conformations That Differ in Reactivity Toward Methyltetrahydrofolate, Adenosylmethionine, and Flavodoxin, *Biochemistry 37*, 5372−5382.
14. Bandarian, V., Pattridge, K. A., Lennon, B. W., Huddler, D. P., Matthews, R. G., and Ludwig, M. L. (2002) Domain Alternation Switches B_{12}-Dependent Methionine Synthase to the Activation Conformation, *Nat. Struct. Biol. 9*, 53−56.
15. Lexa, D., and Saveant, J. M. (1983) The Electrochemistry of Vitamin-B_{12}, *Acc. Chem. Res. 16*, 235−243.
16. Stich, T. A., Brooks, A. J., Buan, N. R., and Brunold, T. C. (2003) Spectroscopic and Computational Studies of Co^{3+}-Corrinoids: Spectral and Electronic Properties of the B_{12} Cofactors and Biologically Relevant Precursors, *J. Am. Chem. Soc. 125*, 5897−5914.
17. Stich, T. A., Buan, N. R., and Brunold, T. C. (2004) Spectroscopic and Computational Studies of Co^{2+}Corrinoids: Spectral and Electronic Properties of the Biologically Relevant Base-On and Base-Off Forms of Co^{2+}Cobalamin, *J. Am. Chem. Soc. 126*, 9735−9749.
18. Pavel, E. G., and Solomon, E. I. (1998) Recent Advances in Magnetic Circular Dichroism Spectroscopy, in *Spectroscopic Methods in Bioinorganic Chemistry* (Solomon, E. I., and Hodgson, K. O., Eds.) pp 119−135, American Chemical Society, Washington, DC.
19. Salmon, R. T., and Hawkridge, F. M. (1980) The Electrochemical Properties of Three Dipyridinium Salts as Mediators, *J. Electroanal. Chem. 112*, 253−264.
20. Zehnder, A. J. B., and Wuhrmann, K. (1976) Titanium(III) Citrate as a Nontoxic Oxidation-Reduction Buffering System for Culture of Obligate Anaerobes, *Science 194*, 1165−1166.
21. Jarrett, J. T., Goulding, C. W., Fluhr, K., Huang, S., and Matthews, R. G. (1997) Purification and Assay of Cobalamin-Dependent Methionine Synthase from *Escherichia coli*, *Methods Enzymol. 281*, 196−213.
22. Amaratunga, M., Fluhr, K., Jarrett, J. T., Drennan, C. L., Ludwig, M. L., Matthews, R. G., and Scholten, J. D. (1996) A Synthetic Module for the *metH* Gene Permits Facile Mutagenesis of the Cobalamin-Binding Region of *Escherichia coli* Methionine Synthase: Initial Characterization of Seven Mutant Proteins, *Biochemistry 35*, 2453−2463.
23. Pol, A., Gage, R. A., Neis, J. M., Reijnen, J. W. M., van der Drift, C., and Vogels, G. D. (1984) Corrinoids from *Methanosarcina barkeri*—The β-Ligands, *Biochim. Biophys. Acta 797*, 83−93.
24. Grahame, D. A. (1989) Different Isozymes of Methylcobalamin: 2-Mercaptoethanesulfonate Predominate in Methanol- *versus* Acetate-grown *Methanosarcina barkeri*, *J. Biol. Chem. 264*, 12890−12894.
25. Harder, S. R., Feinberg, B. A., and Ragsdale, S. W. (1989) A Spectroelectrochemical Cell Designed for Low Temperature Electron Paramagnetic Resonance Titration of Oxygen-Sensitive Proteins, *Anal. Biochem. 181*, 283−287.
26. Drummond, J. T., and Matthews, R. G. (1994) Nitrous Oxide Degradation by Cobalamin-Dependent Methionine Synthase: Characterization of the Reactants and Products in the Inactivation Reaction, *Biochemistry 33*, 3732−3741.
27. Mayhew, S. (1978) The Redox Potential of Dithionite and SO_2 from Equilibrium Reactions with Flavodoxins, Methyl Viologen and Hydrogen plus Hydrogenase, *Eur. J. Biochem. 85*, 535−547.
28. Nilges, M. J. (1979) Electron paramagnetic resonance studies of low symmetry nickel(I) and molybdenum(V) complexes, Ph.D. Thesis, University of Illinois.
29. Stich, T. A., Buan, N. R., Escalante-Semerena, J. C., and Brunold, T. C. (2005) Spectroscopic and Computational Studies of the ATP:Corrinoid Adenosyltransferase (CobA) from *Salmonella enterica*: Insights into the Mechanism of Adenosylcobalamin Biosynthesis, *J. Am. Chem. Soc. 127*, 8710−8719.
30. Stich, T. A., Yamanishi, M., Banerjee, R., and Brunold, T. C. (2005) Spectroscopic Evidence for the Formation of a Four-Coordinate Co^{2+}Cobalamin Species upon Binding to the Human ATP:Cobalamin Adenosyltransferase, *J. Am. Chem. Soc. 127*, 7660−7661.
31. Jarrett, J. T., Choi, C. Y., and Matthews, R. G. (1997) Changes in Protonation Associated with Substrate Binding and Cob(I)-alamin Formation in Cobalamin-Dependent Methionine Synthase, *Biochemistry 36*, 15739−15748.
32. Stich, T. A., Seravalli, J., Venkateshrao, S., Spiro, T. G., Ragsdale, S. W., and Brunold, T. C. (2006) Spectroscopic Studies of the Corrinoid/Iron-Sulfur Protein from *Moorella thermoacetica*, *J. Am. Chem. Soc. 128*, 5010−5020.
33. Kraütler, B., Keller, W., Hughes, M., Caderas, C., and Kratky, C. (1987) A Crystalline Cobalt(II)corrinate Derived From Vitamin B_{12}: Preparation and *X*-Ray Crystal Structure, *J. Chem. Soc., Chem. Commun.*, 1678−1680.
34. Van Doorslaer, S., Jeschke, G., Epel, B., Goldfarb, D., Eichel, R.-A., Kraütler, B., and Schweiger, A. (2003) Axial Solvent Coordination in "Base-Off" Cob(II)alamin and Related Co(II)-Corrinates Revealed by 2D-EPR, *J. Am. Chem. Soc. 125*, 5915−5927.
35. Jarrett, J. T., Drennan, C. L., Amaratunga, M., Scholten, J. D., Ludwig, M. L., and Matthews, R. G. (1996) A Protein Radical Cage Slows Photolysis of Methylcobalamin from *Escherichia coli*, *Bioorg. Med. Chem. 4*, 1237−1246.
36. Schrauzer, G. N., Deutsch, E., and Windgassen, R. J. (1968) The Nucleophilicity of Vitamin B_{12s}, *J. Am. Chem. Soc. 90*, 2441−2442.
37. Schrauzer, G. N., and Deutsch, E. (1969) Reactions of Cobalt(I) Supernucleophiles. The Alkylation of Vitamin B_{12s}, Cobaloximes(I), and Related Compounds, *J. Am. Chem. Soc. 91*, 3341−3350.
38. Chiang, P. K., Gordon, R. K., Tal, J., Zeng, G. C., Doctor, B. P., Pardhasaradhi, K., and McCann, P. P. (1996) *S*-Adenosylmethionine and Methylation, *FASEB J. 10*, 471−480.
39. Svetlitchnaia, T., Svetlitchnyi, V., Meyer, O., and Dobbek, H. (2006) Structural Insights into Methyltransfer Reactions of a Corrinoid Iron-Sulfur Protein Involved in Acetyl-CoA Synthesis, *Proc. Natl. Acad. Sci. U.S.A. 103*, 14331−14336.
40. Liptak, M. D., and Brunold, T. C. (2006) Spectroscopic and Computational Studies of Co^{1+}Cobalamin: Spectral and Electronic Properties of the "Superreduced" B_{12} Cofactor, *J. Am. Chem. Soc. 128*, 9144−9156.

BI700341Y